Long Range, High accuracy Absolute Distance Measurement by Improved Three-Wavelength Heterodyne Interferometry

Pei-Chi Huang,* and Shang-Da Yang,
Institute of Photonics Technologies, National Tsing Hua University, Hsinchu 30013, Taiwan
*Corresponding author: i9xas9966514@gmail.com

Abstract

The complexity and non-ambiguity range (NAR) of the conventional three-wavelength heterodyne interferometry are improved by using one phase modulator and a mapping procedure, respectively. Experiments demonstrated 10-mm NAR and an estimated accuracy of 0.65 nm.

I. Introduction

Accurate positioning over a long range is essential in many applications, such as semiconductor fabrication. Single-wavelength heterodyne interferometry (1λHI) can measure absolute distance with precision in the order of nanometers. However, the non-ambiguity range (NAR) is limited by half-wavelength. A larger NAR can be achieved by using multiple (fixed and/or tunable) wavelengths [1-3] at the cost of increased number of optical frequency modulators (OFMs) and/or slower refresh rate if a wavelength tuning system is used [2,3]. In this contribution, we improved the three-wavelength heterodyne interferometer (3λHI) by using only one OFM (thus simpler lock-in detection), and increased the practical NAR by a new phase point mapping procedure (in place of the conventional multi-step one [2]) that is subject to smaller probability of excessive measurement error. Our experiments demonstrated 10-mm NAR and 0.34-nm accuracy by using three unlocked CW lasers, a common-path geometry for three colors (with interferometric stability), and one electro-optical phase modulator (EOPM).

II. Theory

Fig. 1(a) shows the schematic of a conventional polarization-multiplexed 3λHI using three fixed wavelengths [1,2], where three optical frequencies ν_i, (i=1,2,3) arranged in the form of Fig. 1(b) are modulated by three acousto-optic modulators (AOMs) with three different frequencies f_i,($<<\nu_i$). All the modulated (ν_i+f_i) and unmodulated (ν_i) beams are combined in free space and split into two paths. Three phases ϕ_1, ϕ_3-ϕ_2, ϕ_3-ϕ_1 (ϕ_i=$4\pi d/\lambda_i$ is the phase difference between reference and signal waveforms due to ν_i) are measured by the super-heterodyne scheme [1]. The difference d between the geometric distances of the two interferometer arms is determined by a 3-step estimation procedure (using three manipulated phases $\Phi^{(1)}\equiv(\phi_3-\phi_2)-(\phi_3-\phi_1)$, $\Phi^{(2)}\equiv\phi_3-\phi_1$, $\Phi^{(3)}\equiv\phi_1$) to achieve the maximum NAR (R_{max}=$0.5\times c/\delta\nu$) and the minimum measurement error [$\delta_{d,min}$=$\delta_{\phi1}\lambda_1/(4\pi)$, where $\delta_{\phi1}$ means the error of ϕ_1]. In practice, excessive measurement error ($>>\delta_{d,min}$) occurs for the nonzero phase errors $\delta_{\phi1,2,3}$ could fail the 3-step estimation procedure occasionally. Assume that the three operation wavelengths are λ_1=1531.997 nm, λ_2=1544.580 nm, λ_3=1557.2807 nm (R_{max}=13.3 mm), and $\delta_{\phi1,2,3}$ are independent normally distributed random variables $N(0,\sigma_\phi)$, simulation shows that the standard deviation σ_ϕ<0.16° is required to maintain the probability of excessive error P_ε<1% [Fig. 1(c), open circles].

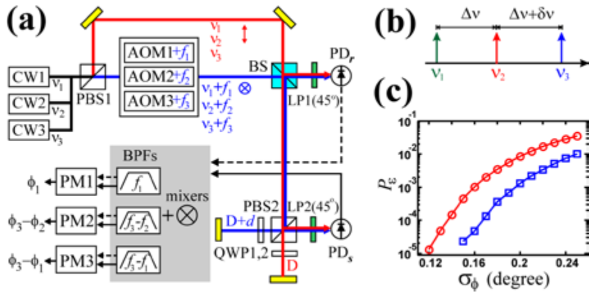

(Fig. 1. (a) Schematic of conventional 3λHI. AOM#: acousto-optic modulator. (P)BS#: (polarization) beam splitter. PD: photodetector. LP: linear polarizer. QWP#: quarter waveplate. BPF: band-pass filter. PM#: phase meter. (b) The arrangements of the three wavelengths used in 3λHI, respectively. (c) Probability of excessive measurement error P_ε versus the standard deviation σ_ϕ of normally distributed phase errors $\delta_{\phi1,2,3}$ for conventional (open circles) and improved (open squares) 3λHI, respectively (assuming λ_1=1531.997 nm, λ_2=1544.580 nm, λ_3=1557.280 nm, 10^6 samplings).

We improve the 3λHI in three aspects (Fig. 2). (1) The three AOMs are replaced by one fiber-pigtailed EOPM [4], enabling (a) elimination of the reference arm (for the driving sawtooth wave can serve the reference of the phase meter), (b) a common-path geometry (with interferometric stability) by using a fiber coupler to combine and split chromatic beams. The inherent phase error due to the wavelength-dependent V_π of the EOPM is effectively suppressed by a calibration procedure. (2) The three wavelengths $\lambda_{1,2,3}$ are separated by a grating to measure the three phases $\phi_{1,2,3}$ simultaneously by a 4-channel phasemeter (one for the reference) using one band-pass filter (BPF). In comparison, the conventional geometry needs mixers and three phase meters (with 3 BPFs and 6 channels in total). Consequently, the new architecture is simpler, more economic, and can be easily extended to more operation wavelengths. (3) A direct mapping procedure replaces the 3-step one to get the desired d. Within an NAR, each d corresponds to a unique "phase point" (ϕ_1,ϕ_2,ϕ_3) and all the phase points form discrete trajectories (due to the modulo-2π limit of ϕ_i) in the 3D space. In the presence of phase error, the measured phase point $(\phi_1', \phi_2', \phi_3')$ is projected onto the nearest trajectory to estimate d. Simulation shows that a relaxed phase error tolerance (σ_ϕ<0.25°) is sufficient to maintain P_ε<1% [Fig. 1(c), squares]. In other words, the phase point mapping procedure permits a larger NAR (smaller $\delta\nu$) for the same 3λHI system (with the same phase measurement error σ_ϕ).

III. Experiment

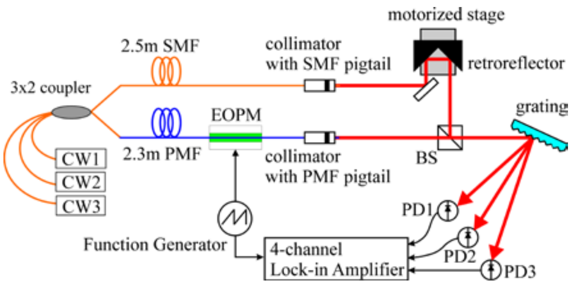

Fig. 2. Experimental setup. SMF: single mode fiber, PMF: polarization maintaining fiber. PD: photodetector. BS: beam splitter. EOPM: electro-optical phase modulator

Fig. 2 shows our experimental setup. A 3×2 fiber coupler combines light from three independent CW lasers operated at wavelengths λ_1=1531.997 nm (195.63 THz), λ_2=1544.580 nm (194.04 THz) and λ_3=1557.2807 nm (192.46 THz), respectively. The combined light is split into two paths, passing through (1) a delay line controlled by a motorized stage with ±20-nm accuracy, and (2) an EOPM driven by a 400-Hz, ±4.75-V sawtooth waveform. The two beams are recombined by a beam splitter (BS), and the three wavelength components are spatially separated by a grating and detected by three InGaAs photodetectors, respectively. The three electric phases $(\phi_1', \phi_2', \phi_3')$ simultaneously measured by a 4-channel lock-in amplifier are processed by a program (in 1 ms) to retrieve the absolute distance. Figure 3(a) shows that the absolute distances d' (dashed) measured by the improved 3λHI differ from the reference distances d_r obtained by 1λHI (with ~3-nm increments, much less the NAR of $\lambda_1/2$) no more than ±0.6 nm (solid) for all the 33,800 sampled distances spanning over 100 μm. There is no excessive error and the standard deviation σ_d of the differences δ_d=d'-d_r is 0.19 nm. Since the reference distances d_r may have some error as well, we estimate the accuracy of d' by the simulation result of Fig. 1(d). In view of the fact that the probability of excessive measurement error P_ε is less than $(33{,}800)^{-1}$, we estimate the standard deviation of the phase error as $\sigma_{\phi 1}$<0.153°. Since the distance error δ_d is related to the phase error $\delta_{\phi 1}$ via a linear relation $\delta_d=\delta_{\phi 1}\lambda_1/(4\pi)$, δ_d is also a normal random variable with standard deviation $\sigma_d=\sigma_{\phi 1}\lambda_1/(4\pi)<$ 0.33 nm. The accuracy (95% confidence interval) becomes twice the standard deviation $2\sigma_d$<0.65 nm. To confirm the long NAR, we calibrated the stage displacements by recording the interferometric intensity due to λ_1 on the fly. The stage stopped for 120 s at each of the 5 positions, during which the absolute distance was measured by 3λHI at a refresh rate of 33 Hz. The resulting values d' are compared with the reference distances d_r obtained by interferometric fringe counting. As shown in Fig. 3(b), d' and d_r are in good agreement (σ_d <340 nm) for all the 5 absolute distances spanning over 10 mm. Note that the larger σ_d (compared to the 0.19 nm of the previous test) is dominated by the path length fluctuation within the 120-s data acquisition time due to environmental perturbation, instead of the measurement error.

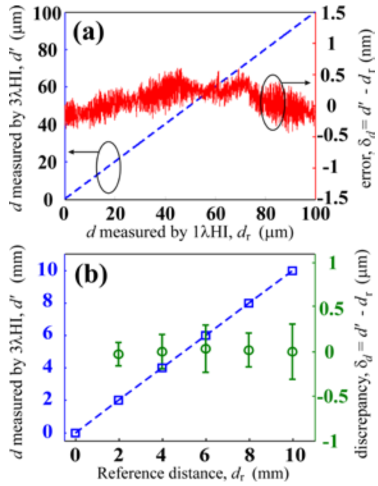

Fig. 3. (a) Absolute distances measured by 3λHI versus those measured by 1λHI (dashed), and the difference between them (solid). (b) Absolute distances measured by 3λHI versus those measured by interferometric fringe counting (open squares), and the difference between them (open circles). Each error bar means the standard deviation σ_d of the 4,000 discrepancy values.

IV. Conclusion

The complexity and NAR of conventional 3λHI are improved by using one (instead of three) phase modulator and a phase point mapping procedure, respectively. The improved geometry can be easily extended to more operating wavelengths (provided by laser comb) such that NAR in the order of meters can be achieved under practical phase error. This work was supported by the National Science Council in Taiwan under grants NSC 100-2221-E-007-093-MY3 and 99-2120-M-007-010.

References

[1] R. Dändliker, R. Thalmann, and D. Prongué, "Two-wavelength laser interferometry using superheterodyne detection", *Opt. Lett*, **13**(5), pp. 339-341 (1988).

[2] R. Dändliker, Y. Salvadé and E. Zimmermann, "Distance measurement by multiple-wavelength interferometry", *J. Opt*, **29**(3), pp. 105-114 (1998).

[3] Y. Salvadé, N. Schuhler, S. Lévêque, and S. L. Floch, "High-accuracy absolute distance measurement using frequency comb referenced multiwavelength source", *Appl. Opt*, **47**(14), pp. 2715-2720 (2008).

[4] D. C. Su, M. H. Chiu and C. D. Chen, "A heterodyne interferometer using an electro-optic modulator for measuring small absolute distances", *J. Opt*, **27**(1), pp. 19-23 (1996).